On the Immobilized Polymer Fraction in Attractive Nanocomposites: T g Gradient versus Interfacial Layer

Carlos Fernandez-De-Alba, Andrew Jimenez, Mozhdeh Abbasi, Sanat Kumar, Kay Saalwächter, Guilhem P. Baeza

On the Immobilized Polymer Fraction in Attractive Nanocomposites: T_g Gradient vs. Interfacial Layer

Carlos Fernandez-de-Alba,[1] Andrew M. Jimenez,[2] Mozhdeh Abbasi,[3] Sanat K. Kumar,[2] Kay Saalwächter[3,*] and Guilhem P. Baeza[4,*]

kay.saalwaechter@physik.uni-halle.de, guilhem.baeza@insa-lyon.fr

[1] Univ Lyon, INSA-Lyon, CNRS, IMP, UMR 5223, Service RMN Polymères de l'ICL F-69621, Villeurbanne, France

[2] Department of Chemical Engineering, Columbia University, New York, New York 10027, USA

[3] Institut für Physik, Martin-Luther-Universität Halle-Wittenberg, D-06099 Halle (Saale), Germany

[4] Univ Lyon, INSA Lyon, UCBL, CNRS, MATEIS, UMR5510, 69621, Villeurbanne, France

---

Abstract: We study the slowing down of polymer dynamics in canonical nanocomposites made of strongly interacting mixtures of polyvinyl-pyridine (P2VP) and silica nanoparticles (radius R=7 ± 2 nm) by means of low-field NMR relaxometry. We demonstrate that this technique enables the accurate quantification of the fraction of immobilized (irreversibly adsorbed) polymer on to the filler surface, in a manner that complements data from broadband dielectric spectroscopy (BDS) and differential scanning calorimetry (DSC). We rationalize the slowing down by using two previously developed approaches to model the immobilized layer. The first one is based on a glass transition temperature, T_g, gradient, while the second one assumes a single interfacial component with a distribution of relaxation times. While both models convincingly fit the NMR data providing us with robust and complementary conclusions, the former approach is found to fit more accurately previously published DSC experiments. Quantitatively, NMR results indicate that the segmental relaxation of the immobilized layer is ca. 1 decade slower than in the bulk polymer while earlier BDS analyses were equivocal on this point, indicating either 1 or 2 decades. These discrepancies highlight the difficulties and potential model dependencies in quantifying the dynamics of the minority polymer fraction in the immobilized layer, necessitating a systematic multi-technique approach to properly characterize dynamical heterogeneities in polymer-based materials.

1. Introduction

Polymer based nanocomposites (PNCs) have attracted considerable interest due to their ability to significantly enhance the physical properties of polymers, *e.g.,* mechanical, optical and electrical properties.[1,2,3,4] A well-known example concerns the application of PNCs in tires where the addition of nanoparticles improves the wear resistance while diminishing the vehicle's fuel consumption.[5] Such properties enhancements have been assumed to be governed by an immobilized layer comprised of polymers that are essentially irreversibly bound to the nanoparticles (NPs) surface; with increasing NP loading, these layers percolate through the sample to form a network that significantly alters PNC macroscopic properties.[6]

Among all nanofilled polymers, "attractive nanocomposites" made of a strongly interacting polymer-filler combination have been particularly investigated for their ability to form strong networks resulting in complex dynamics. A particularly notable case is of poly-2-vinyl pyridine (P2VP) filled with nano-silica where the two components interact favorably through multiple hydrogen bonds ensuring individual particle dispersion.[7] The resulting network, based on silica NPs bridged by P2VP strands, was shown to noticeably increase the shear modulus of the material by more than two orders of magnitude when filled with ca. 30 vol.% (50 wt.%) of 14 nm diameter nanoparticles.[8,9] In contrast, the reinforcement in non-attractive nanocomposites (*e.g.* tires) filled with a similar fraction of nano-objects is limited to a factor of 20-30, *i.e.*, 5-10 times less than the attractive case.[10,11] This difference in behavior is assigned to the immobilized (or interfacial) layer surrounding the NPs in the attractive case. This ensures stress transmission through "glassy bridges",[8] *i.e.*, through adjacent polymer domains of slow segmental (or "α") dynamics. This "interfacial" layer must be distinguished from the "bound" layer which refers to a larger polymer sub-ensemble made of chains segments connected to the particles but located far enough from them not to have their average segmental motion perturbed.[12] The bound layer however has a major role on longer time dynamics such as those probed with rheology.[9] Other authors found similar trends in other nanocomposites.[13]

The presence of the immobilized layer was further evidenced through differential scanning calorimetry (DSC)[9,14] and broadband dielectric spectroscopy (BDS).[7,9,14,15,16] Both of those methods revealed a clear broadening of the "calorimetric" glass transition and segmental relaxations with increasing the filler content, respectively. A seemingly well-separated slower relaxation mode (α') was also observed by Cheng et al. with BDS.[17] In similar systems, Holt et al. rationalized the broadening of the segmental relaxation through a bicomponent Havriliak-Negami function representing the contributions of the neat matrix (α) and a more sluggish interfacial layer (α'). [14] This approach is consistent with a fraction of polymer with reduced-mobility shifted in timescale by about two decades, but with a similar activation energy as the neat P2VP. In contrast, in the context of a different study, the same group analyzed new BDS data on virtually the same samples and concluded that the slowing down of the interfacial layer was one decade only.[16] This quantitative contradiction, *i.e.*, the one or two decades dynamical slow down, illustrates that BDS, although having a large dynamic range, may suffer from significant fitting ambiguities.

In the same vein, while the interfacial polymer fraction (or corresponding interfacial layer thickness) was also determined from BDS measurements by using the amplitude of the α' process, *e.g.*,[14,17,18]), we acknowledge that its estimation is severely challenged by the presence of the interfacial polarization mechanism known as "Maxwell-Wagner-Sillars" (MWS). Because this phenomenon depends not only on the NPs structure and their surface chemistry, but also the nature and (temperature dependent) diffusion coefficient of the charge carriers within the PNC, it is hard to quantify. This makes the joint fitting of the real and imaginary part of the electric permittivity (respectively denoted ε' and ε'') equivocal at best.

Beyond quantitative estimations of the dynamical slow down and fraction of immobilized layer, the present work addresses the more fundamental question of whether the immobilized layer should be treated from a continuous or a bi-component approach. This question can be

illustrated by the following example. By using BDS on similar nanosilica/P2VP composites, Holt et al. [14] and later Baeza et al. [9] measured a similar broadening of the segmental relaxation with increasing the filler fraction. However, while in the former case the authors used a bi-component approach (α and α_2) to fit the imaginary part of the electric permittivity, a continuous broadening of the α relaxation was considered in the latter case in addition to an MWS process. This resulted in two different pictures being respectively (i) a distinct interfacial layer characterized by a segmental relaxation 10-100 times longer than the bulk's one, and (ii) a continuous slowing down of the polymer chains quantified by the drop of the "symmetric exponent" in the Havriliak-Negami function (denoted γ in ref.[9]), providing a quasi-identical average segmental relaxation time regardless of the filler content. While, both scenarios seem reasonable and well-argued, the best option is difficult to identify because of the presence of the MWS contribution, requiring therefore an alternative experimental technique.

Similar studies were conducted on poly-vinyl acetate (PVAc)[17,18] and poly-ethylene-acrylate (PEA)[19,20] based PNCs. These works verify the presence of an immobilized polymer layer at the filler surface, one that is characterized by strongly retarded dynamics. In ref.[19], Papon et al. used low-field nuclear magnetic resonance (LF-NMR) to extract both the fraction and the dynamics of such immobilized chains (then termed "glassy layer", a term we henceforth avoid). In this work, the material was subdivided into three components, a mobile bulk material, an intermediate and a strongly immobilized polymer fraction, respectively; the latter two constitute the reduced-mobility fraction. A significant advantage of NMR is that its signal is strictly proportional to the number of protons, thus allowing us to "count" monomers, and avoid some of the ambiguities of BDS (see above). Further,[20] combining NMR and DSC data allowed the authors to prove that both sets of results were consistent with a continuous gradient in T_g, such as imagined originally by Keddie and Jones,[21] for the PEA silica composites:

$$T_g(h) = T_g^{\infty}\left[1 + \left(\frac{\delta}{h}\right)^{\beta}\right] \quad (1)$$

where h is the distance from the particle surface, δ is the characteristic length of the gradient that must not be understood as the interfacial layer thickness, T_g^{∞} is the glass transition temperature in the bulk and β describes the gradient shape. Note that this model should be considered simplified because it implies that other parameters in the Vogel-Fulcher equation describing the temperature dependence of the dynamics are unchanged (*i.e.*, the h-dependence of the segmental relaxation times is taken to be T-independent). In addition, the cited work was subject to the more significant limitation that there is a relatively thick 1-2 nm base layer of the silanization agent on the NPs, which is treated as the inner shell before the onset of the T_g gradient in the PEA. Here, we focus on the P2VP silica model nanocomposites, which do not contain any additional components (apart from a small amount of antioxidant). Relying on the "proton counting" feature, we use NMR in conjunction with DSC as unbiased approaches for quantifying the material with reduced-mobility and test whether the T_g gradient or single interfacial layer models can best describe the data.

2. Materials and Methods

Nanocomposite preparation

PNC samples (loaded with 10, 30 and 50 wt.% in silica corresponding respectively to volume fractions Φ = 6, 18 and 31 vol.%) were prepared following the protocol used for the samples studied by BDS in ref.[9]. Thermogravimetric analysis data is provided in Supporting Information (SI) section 1. Hydrophilic silica nanoparticles (radius R=7 ± 2 nm) were donated by Nissan Chemical Corporation, USA (MEK-ST). Methyl ethyl ketone (MEK, or 2-butanone, ACS reagent >99.0%) and pyridine (anhydrous, 99.8%) were purchased from Sigma-Aldrich, GER. The 100

kDa P2VP (purchased through Scientific Polymer Products, USA) was dissolved overnight in MEK at a concentration of 50 mg mL^{-1} together with a small amount of Irganox antioxidant (BASF, GER) (≈0.5 wt.% with respect to the polymer). The NPs, stabilized by the manufacturer in MEK, were mixed with pyridine at a ratio of 4:1 and sonicated for 10 minutes before being added into the polymer solution. The mixture was then vortexed for one hour and cast at room temperature in a Teflon dish for three days. Annealing was performed at 150 °C in a vacuum oven for five days prior to any testing. Transmission Electron Microscopy (TEM) was performed on a JEOL 1400 Flash microscope at 120 keV on samples ultramicrotomed at room temperature. Micrographs in Figure 1 confirm uniform NP dispersion at all filler contents considered. Small angle X-ray scattering (SAXS) on low loading samples confirm uniform NP dispersion (not shown here, see ref.[7]). An additional vacuum drying step was used at 80 °C for 12 hours before the NMR experiments were conducted.

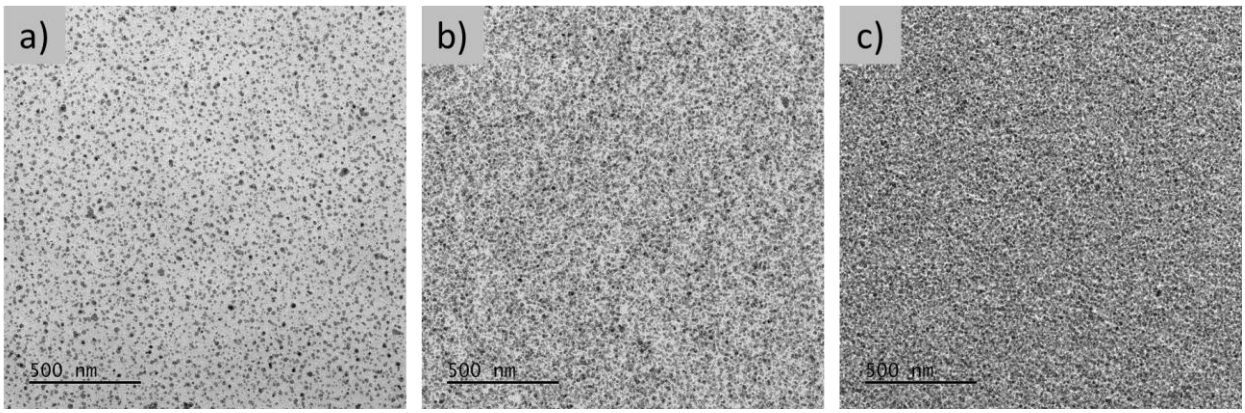

Figure 1: Transmission electron micrographs of PNCs loaded with a) 6, b) 18 and c) 31 vol.% in silica. Black bars are 500 nm.

Low-Field NMR

NMR measurements were performed on a Bruker Minispec mq20, at a 20 MHz proton resonance frequency. The temperature was lowered from 473 K to 403 K with a BVT 3000 heater

working with nitrogen gas (the glass transition temperature of P2VP is T_g=373 K). Prior to each measurement, the temperature was stabilized for 10 minutes. The experiments were then repeated from low to high temperature to insure data reproducibility. Neat P2VP was further measured down to 313 K to extract M_2, the second moment of the dipolar-broadened NMR spectrum (see Equation 3 in section 3 and SI section 2).

In this work, we choose to use a methodology previously followed by others combining free induction decay (FID) and magic sandwich echo free induction decay (MSE-FID) pulse sequence.[19] While FID was acquired with a single π/2 excitation, the accurate fitting of the rigid component fraction (immobilized polymer) is challenged by the dead time (15 μs) inherent to the technique. To solve this issue, we refocused the strong dipolar interactions (fast decay contributions) by using the MSE-FID sequence.[22] This signal suffers some intensity loss, but also allows for an accurate fitting of the most rigid components. For all the materials, both FID and MSE-FID signals at short times were adjusted to be between 60 and 100 % intensity and limited to 200 μs to avoid any field inhomogeneity which might affect the signal at longer acquisition times. Importantly, the gain was identical for both FID and MSE-FID experiments.

3. Results and Discussion

3.1 Preliminary considerations on the interfacial layer from DSC results.

Figure 2a shows our previous data on a PNC loaded with 31 vol.% in silica, where modulated DSC was used to quantitatively determine the temperature-dependent heat capacity of the PNCs.[9] The plotted data is obtained by subtraction of the silica contribution (with known and near-linear temperature dependence) around the region of the P2VP glass transition. The plot also shows the T_g step for neat P2VP, which is the "base function" from which the fits to the trace of the PNC was constructed. For each assumed contribution (*i.e.*, spherical shell) with shifted T_g,

the neat response was shifted by the required ΔT_g, not just along the x-axis but along a line with the slope defined by the glassy-state heat capacity, *i.e.*, the slope of the initial part of the P2VP trace.

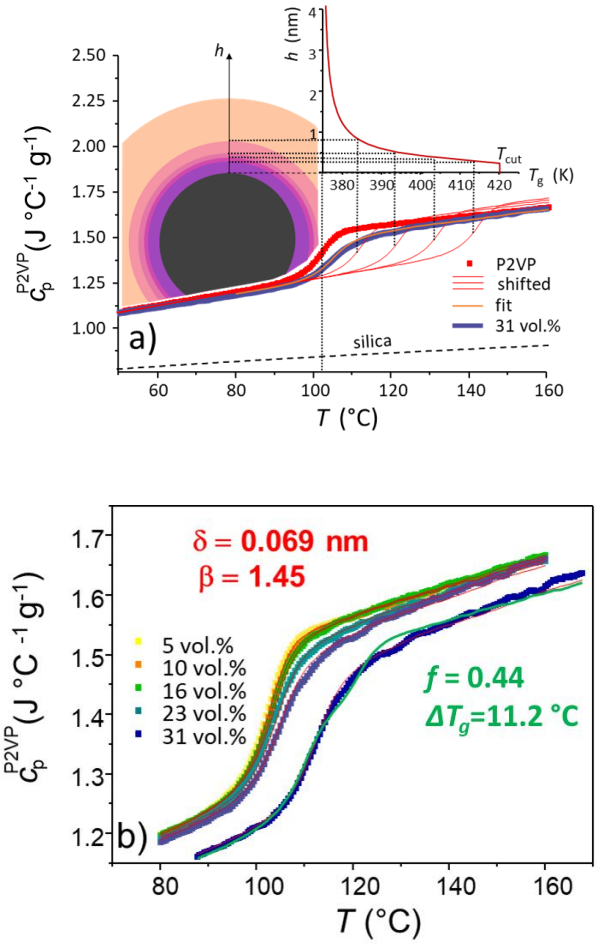

Figure 2: a) Modulated DSC data adapted from ref.[9] (heat capacity of the neat P2VP and polymer phase in nanocomposite filled with 31 vol.% in silica). Thin solid lines are shifted version of the neat P2VP measurement and illustrate the gradient in T_g around the nanoparticle. b) Analogous data (5 vol.% to 31 vol.%) from global fit with the T_g gradient model (thin red solid lines) providing δ =0.069 nm and β=1.45. Data for 31 vol.% composite is shifted for clarity; the thick green solid line is a fit based on the interfacial layer model.

The inset of Figure 2a shows the implementation of the T_g-gradient shell model of Papon et al.,[20] where T_{cut} is the highest glass transition temperature for the immobilized layer associated with the material in direct contact with the surface. In this work, the authors only demonstrated the qualitative agreement of predicted DSC data of the composite based upon the gradient parameter extracted from NMR measurements. We here go beyond the previous analysis by doing a least-square fits to the DSC response, which turned out to be possible and robust. The model has two fitting parameters, which are the gradient length scale δ and the exponent β (Papon et al. restricted their analyses to β =1). All other parameters of the model, which are the volume fractions of the shells in a finite-step integration are known via the given silica volume fraction and the particle size (R = 7 nm). For fixed β =1, we obtained δ values between 0.01 and 0.02 nm for increasing silica fraction, where the result for larger fractions must be considered more reliable due to the larger deviations from neat P2VP (see, *e.g.*, Figure 5a). We observed a significant improvement of fitting quality by allowing β to vary freely. A simultaneous fit to all data sets (5-31 vol.% loadings), shown in Figure 2b, provides the best-fits results in the same figure. The T_g gradient corresponding to the so-obtained δ and β values, respectively 0.069 nm and 1.45, is the one shown in the inset of Figure 2a (calculated from Equation 1).

In Figure 2b we also show a shifted version (for clarity) of the data for the 31 vol.% sample that we fit assuming the simple superposition of the neat response and a single T_g-shifted component (solid green line). This fit, which is based on a relatively simpler approach, is visually inferior, particularly regarding the overestimation of c_p at the glass transition endpoint and its slope at higher temperature. We thus conclude that the sample is unlikely to contains two actual fractions with well-separated T_g as suggested on the basis of BDS data in several publications - see *e.g.* ref. [14,17,18] by Sokolov et al. Given these facts we believe it is not appropriate to describe the BDS data, taken at higher temperature, where the segmental relaxations are faster and presumably more homogeneous (diffusion-averaged), with two distinct components. We note

that the width of the BDS-detected second alpha relaxation (α") in the nanocomposites is not significantly wider than the one for the main α relaxation (see *e.g.*, ref. [14]).

3.2 Analysis of the neat P2VP from low field NMR

In Figure 3a, we present the evolution of the free induction decay signal "FID" (I_{FID}) measured on the neat P2VP as a function of the NMR time for temperatures varying from 403 to 473 K. As expected, a slower signal decay is observed at high temperatures, *i.e.*, when the chains have extra-mobility (short segmental relaxation time); steeper decays indicate more sluggish dynamics corresponding to slower segmental relaxations. In addition to the FID signal, Figure 3b shows the magic-sandwich-echo free induction decay signal "MSE-FID" (I_{MSE}) which allows us to measure the material's response at times shorter than the spectrometer dead time (ca. 15 μs). Due to T_2-relaxation effects during the MSE-FID measurement, I_{MSE} is somewhat reduced, and goes through a minimum when the segmental correlation time is of the order of the inverse static limit dipolar coupling (see inset). This method thus probes a somewhat smaller dynamic sub-ensemble, which can be quantified from the measured relative intensities. This fact is considered in our fits.

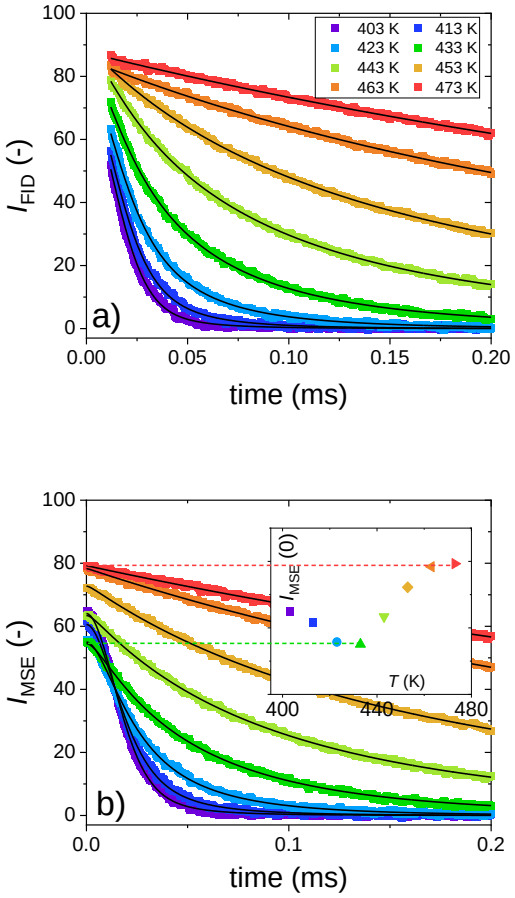

Figure 3: a) Raw $I_{FID}(t)$ signal measured from the neat P2VP between 403 and 473 K. b) Analogous data for $I_{MSE}(t)$. Solid lines represent joint fits to the data (I_{FID}, I_{MSE}) for each temperature with the AW function (Equation 3) considering a log-normal distribution of τ_c (see text). The inset shows the expected non-monotonic variation of the MSE-FID signal at short time with the temperature (see refs. [19,20]).

The calorimetric glass transition temperature (T_g) of P2VP is ≈373 K. However, glass transition effects on the NMR observables only set in several tens of degrees higher (typically from T_g+30 °C) , *i.e.*, when the segmental dynamics reaches correlation times (α-relaxation times) τ_c of 0.1-

0.01 ms, corresponding to the range where it is of the order of the inverse of the average dipolar coupling constant in the static limit (i.e., $\approx 2\pi \times 30$ kHz).[20]

Unlike in BDS, the relationship between the measured NMR response and the timescale of segmental relaxation is highly non-linear, and all available theories involve approximations, rendering the extraction of τ_c semi-quantitative. However, the fact that we are able to represent the neat-polymer data quantitatively at any given temperature means, that we will be nevertheless be able to evaluate quantitatively the amount of reduced-mobility material and the degree of slowdown in our nanocomposites (section 3.3).

As mentioned, the decay of the NMR signal (the "apparent" T_2 relaxation time) reflects the strength of through-scape dipolar couplings, which become averaged out due to segmental motion when it is fast enough to interfere with the distance- and orientation-dependent dipolar-coupling effect. We thus detect motions through any change in dipolar couplings in the dense proton system, arising from either rotations of internuclear vectors (both intra- and inter-segmental) or changes in distance (by actual diffusing or by rotation of a neighboring segment). Given the featureless data, it is impossible to disentangle these contributions. Assuming rather simplistically that these effects are governed by a single correlation time τ_c, the I_{FID} and I_{MSE} were simultaneously fitted with the Andersen-Weiss (AW) function, originally developed for use in electron paramagnetic resonance,[23] and successfully used recently to model NMR data [19,20,24] - parameters are defined below:

$$I(t,T) = I_0\, exp\left\{(-0.5\, S^2 M_2 t^2)\, exp\left[-(1-S^2)M_2\tau_c^2(T)\, \left(exp\left(-\frac{t}{\tau_c(T)}\right)+\frac{t}{\tau_c(T)}-1\right)\right]\right\}. \qquad (2)$$

This model includes the option for locally anisotropic (*e.g.* uniaxial) dynamics as quantified by the order parameter $S = \langle P_2 \rangle$. Indications of anisotropic dynamics in the interfacial layer were recently discussed by Sokolov and coworkers[12] based on works by Liu et al.[25] and Ou-Yang et al.[26] evidencing that the most probable conformation of an adsorbed chain is a pan-cake like

structure. This option, which is further discussed in Section 3.3.1., was used to perform the fits of our composites' NMR data by varying S from 0 to 0.3 as illustrated in Figure 8, resulting in no major impact on the $\tau_c$value. For example, applying Equation 2 within the IFL model (see section 3.3.1) to fit data of the nanocomposite loaded with 50 wt.% at 453 K resulted in τ_c =6.8 μs and 4.9 μs for S=0 and S=0.3 respectively (with fixed σ=0.5, see Equation 4).

Besides, when S=0, *i.e*, in the case of isotropic dynamics (considered true for the neat matrix), Equation 2 simplifies into:

$$I(t,T) = I_0\, exp\left\{-M_2\tau_c(T)^2\left[\, exp\left(-\frac{t}{\tau_c(T)}\right) + \frac{t}{\tau_c(T)} - 1\,\right]\right\} \tag{3}$$

In Equations 2-3, the instrument related prefactor I_0 and the apparent correlation time τ_c were the (unshared) fitting parameters. M_2 is the second moment of the dipolar-broadened spectrum, which is a measure of the average static low-temperature limit dipole–dipole coupling D_{HH} in the system, $M_2 \approx \left(\frac{9}{20}\right) {D_{HH}}^2$. Even without motion, this quantity decreases upon heating due to thermal expansion (SI section 2 for details on its determination). Upon heating, the segmental relaxation time decreases, and when it reaches a value of about $1/2\pi D_{HH}$, *i.e.*, about 10 μs, the mentioned averaging effects set in and the decay of the observed relaxation function $I(t,T)$ starts to lengthen (the effective transverse relaxation time starts increasing). Note that a τ_c of 10 μs is usually found above T_g+ 30 K (while it is 100 s at T_g). In this range, τ_c can be fitted stably and values for higher temperatures were estimated by extrapolation (see SI section 2). In addition, τ_c was systematically assumed to follow a log-normal distribution $P(\tau)$,

$$P(\tau) = \frac{1}{\sqrt{2\pi\sigma^2}} exp\left(\frac{-\big(ln\,(\tau) - ln(\tau_c)\big)^2}{2\sigma^2}\right) \tag{4}$$

where the logarithmic standard deviation σ was a fit parameter. We found that the resulting σ were very similar for the I_{FID} and I_{MSE} signals – for the neat P2VP it varies systematically from

0.50 to 0.88, from 403 to 473 K. Accordingly, τ_c values were found to vary from 27.2 μs to 0.3 μs for I_{FID}, and from 28.6 μs to 0.133 μs for I_{MSE}, showing the consistency of our dual data set. This minimal model provides a near-perfect fit to the data, which serves the important purpose of parametrization/interpolation of bulk P2VP data beyond a possible interpretation of the fit parameters. While the single-τ_c assumption is unrealistic in the light of the complex relaxation map of P2VP (see below), it is not possible to use a more complicated model for fitting without challenging a robust fit. The question of the molecular-level origin of the so-observed relaxation actually opens opportunities for future experimental investigations. In fact, we envision dual BDS vs. LF-NMR analyses performed on series of model polymers in which the relative amplitude and/or the relaxation time of segmental and local processes could be varied progressively. This philosophy was notably used in the past to investigate series of methacrylate-based polymers where the length of the side group was correlated in a systematic way with the segmental relaxation and nano-structuration by means of BDS, DSC and mechanical spectroscopy,[27] as well as neutron spin echo.[28] Also, selective deuteration of the side groups is certainly of great interest in this context, enabling to discriminate contributions coming from segmental or local motions on the apparent "τ_c relaxation" by using LF-NMR only.

We can now compare the values of τ_c with the P2VP segmental relaxation time (τ_α) obtained from BDS, as well as with the rheological shift-factor at the appropriate reference temperature, a_T.[9] This comparison is reported in Figure 4a, where reasonable agreement is observed between the three techniques, yet noting a shift towards too-large τ_c at higher temperatures and an apparently lower apparent activation energy for the NMR data at low temperature, resulting in a seemingly Arrhenius-type trend. To understand these deviations, we stress again the simplicity of the AW model, notably through (i) the assumption of an exponential loss of orientation correlation, (ii) the log-normal distribution of segmental relaxation time and (iii) the slight temperature dependence of M_2. These issues will impart systematic errors on the fitted τ_c.

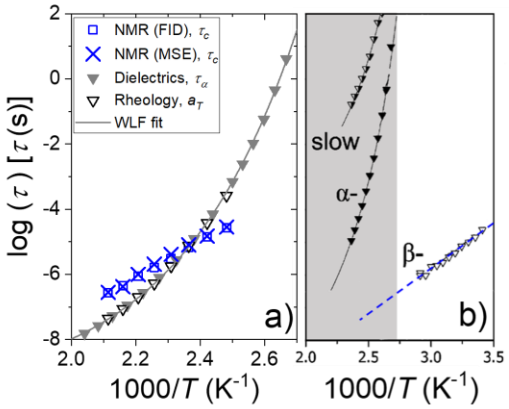

Figure 4: Temperature dependence of the neat P2VP segmental relaxation time. Panel a) shows date from our previous publication probed by dielectric spectroscopy (τ_α) and rheology (a_T),[9] together with the low-field NMR (τ_c). The solid line is a fit of the dielectric data based on the WLF model at a reference temperature of 373 K. Panel b) shows dielectric data for a high molecular weight P2VP ($\overline{M_n}$ ~ 30 kDa) adapted from ref.[29] – see details in the text, with the grey shaded region indicating the temperature range in a).

Beyond this inherent uncertainty, the two discrepancies can be qualitatively understood in view of the complexity of the relaxation processes in P2VP. Figure 4b shows results from a more complete analysis of dielectric data.[29] It is a processed version of Figure 6 of this reference, scaled to match the representation in Figure 4a. In addition to the α relaxation, there is a slower process related to the glass transition and attributed to a final isotropization of monomer sequences following a partly anisotropic α process, in analogy to earlier observations on poly(n-alkylmethacrylates) claiming a "conformational memory.[30] In addition, there is a β process associated with the pyridine ring (possibly π flips). Now, Equations (2,3) imply significant changes of the NMR signal when τ_c is in the range of 1 to 100 μs. The additional processes feature broad correlation time distributions,[29] such that they must be expected to contribute in

this dynamic range, thus biasing the fitted τ_c and explaining qualitatively the deviations from τ_α. Importantly yet, the main contributor to τ_c is the segmental relaxation, such that in the high-temperature range, where its temperature dependence is reflected correctly, we can expect to obtain a good estimate of the extent of slowdown in the nanocomposite samples. Finally, we remind that the most important purpose of using Equations (2-4) is the parametrization/interpolation of the measured data, used below primarily for a reliable quantification of the amount of interfacial material.

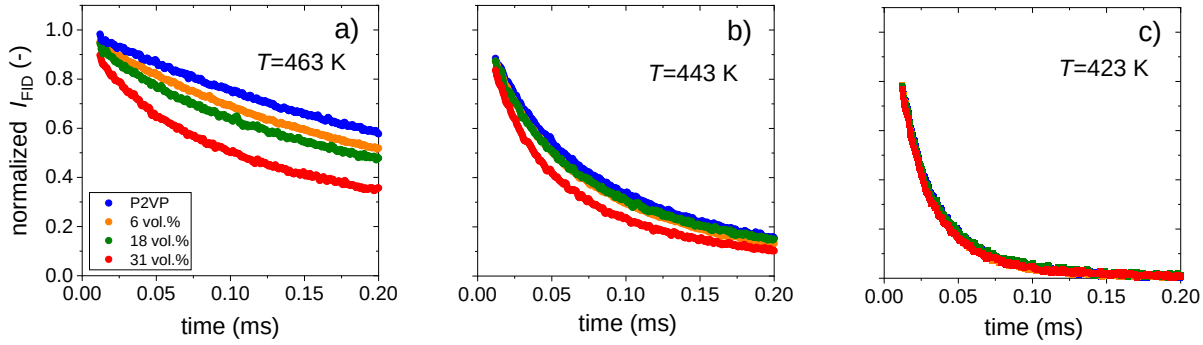

Figure 5: Normalized I_{FID} signals for the net P2VP and the nanocomposites loaded with 6, 18 and 31 vol.% in silica measured at a) 463 K, b) 443 K and c) 423 K. Intensity normalization is performed by using the zero-time limit from the IFL model fit as shown in Figure 6.

3.3 Impact of the silica loading on P2VP dynamics

Based on the preliminary results obtained on neat P2VP as a reference, our aim is to quantify the impact of the silica loading on polymer dynamics. Two quantities are particularly targeted here: (i) the fraction of P2VP adsorbed onto the silica surface (denoted by f below), and (ii) the change of the segmental relaxation time of the immobilized layer, or in other words, its dynamical shift with respect to the bulk P2VP. Normalized I_{FID} data obtained from the neat P2VP and the nanocomposites loaded with 6, 18 and 31 vol.% silica are shown in Figure 5, where the

immobilized layer contribution (faster decay, *i.e.*, shorter T_2) clearly appears at high temperatures, *i.e.*, far from the bulk P2VP glass transition (Figure 5a). Conversely, when measuring at lower temperature, the NMR signals from the PNCs tend to collapse progressively onto the neat matrix response indicating that the whole polymer phase is becoming glassy from an NMR point of view (Figure 5b-c). For this reason, we restricted the fitting procedures below to the 433-473 K range, in which a reasonable distinction could be made between the bulk and the interfacial layer dynamics.

While the signals from the PNCs loaded with 6 and 18 vol.% in silica are rather close over the whole temperature range, the 31 vol.% sample signal appears much stiffer from an NMR point of view, indicating a significantly higher f. This variation parallels the initially limited, then stronger broadening of the α-relaxation observed in BDS when increasing the filler content.[9,14] Also, it is reminiscent of a similar WLF trend of the rheological shift factor in PNCs loaded with $\Phi \leq$10 vol.% before a clear transition towards an Arrhenius-like behavior at higher filler content.[9] (For the sake of completeness, the whole data set containing all the temperatures and filler fraction dependences of both I_{FID} and I_{MSE} signal is provided in SI section 3).

3.3.1. NMR data fitting with the single Interfacial Layer (IFL) model

The interfacial model consists of adding the bulk P2VP contribution (determined in the previous section) to an AW term (described in Equation 2-3) for the immobilized layer.

$$I_{FID,MSE}(t,T) = (1-f)\, I^{P2VP}_{FID,MSE}(t,T) + f\ I^{IFL}_{FID,MSE}(t,T)\,, \qquad (5)$$

f is the fraction of immobilized layer; $I^{P2VP}_{FID,MSE}$ and $I^{IFL}_{FID,MSE}$ being, respectively, the AW fit performed on the matrix data (black lines in Figure 3) and the additional contribution from the immobilized layer. Note that Equation 5 assumes that FID data are normalized to 1 at short time while MSE-FID ones are systematically lower by a factor $I_{FID}(0)/I_{MSE}(0)$ that depends on the

temperature (see the inset of Figure 3b). This method applied jointly on I_{FID} and I_{MSE} enables a straightforward and joint evaluation of f and τ_c thus limiting the number of fit parameters. The result of this approach (considering S=0) is presented in Figure 6 together with the T_g gradient model (see next section) on a nanocomposite filled with 31 vol.% in silica at 453 K, highlighting a large contribution of the immobilized layer with respect to the bulk.

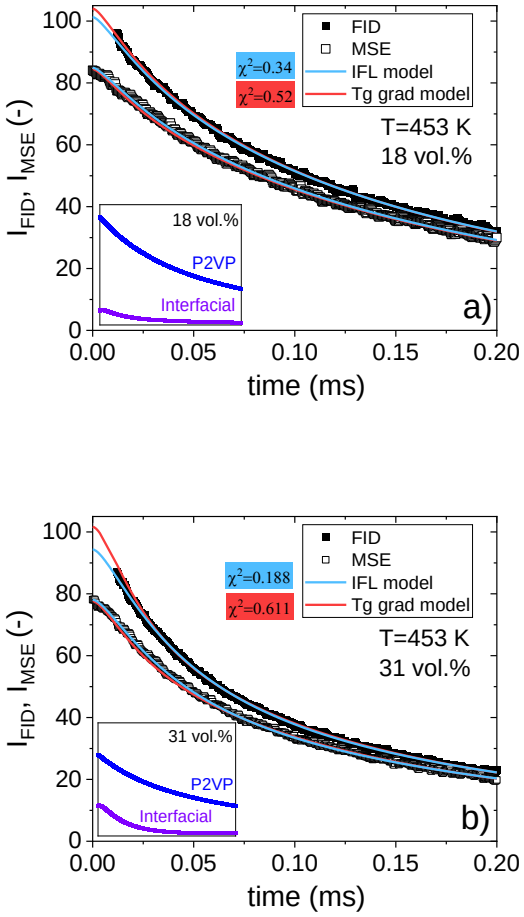

Figure 6: I_{FID} and I_{MSE} raw signals measured at T=453 K. Light blue and red solid lines stand respectively for the IFL and the T_g gradient models. a) Nanocomposite loaded with 18 vol.% and b) 31 vol.%. The insets represent the FID contributions of the bulk P2VP and the interfacial layer from the IFL model.

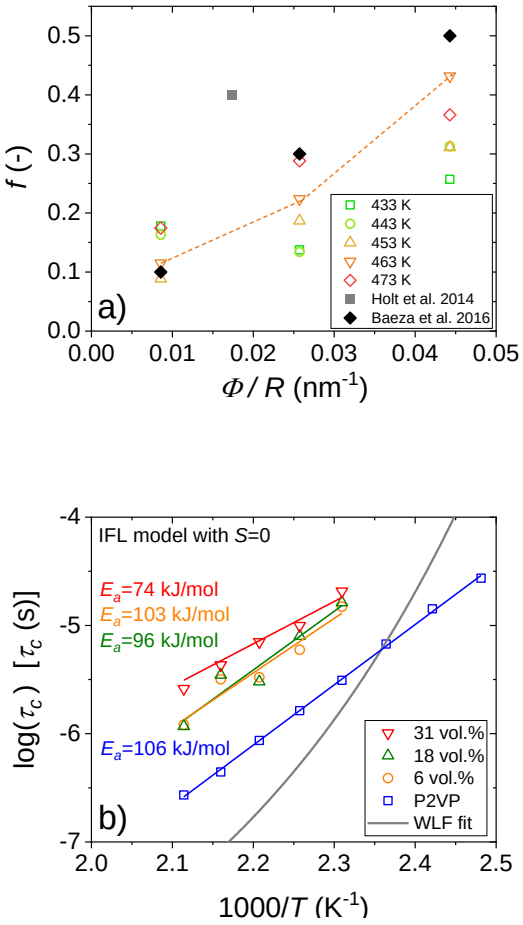

Figure 7: a) Fraction of immobilized layer extracted from FID experiments performed between 433 and 473 K on composites loaded with 6, 18 and 31 vol.% in silica as a function of the reduced filler fraction Φ/R representing the total interfacial surface. BDS based data from Baeza et al. (2016) and Holt et al. (2014) are shown for comparison. The dashed line is a guide to the eye connecting the 463 K data. b) Segmental relaxation time as function of the reciprocal temperature for the neat P2VP and the immobilized phase in nanocomposites of various filler content. τ_c values are extracted from FID data (MSE-FID ones are almost identical). The solid gray line is the same WLF law as in Figure 2. Other solid lines are linear fit to the data to extract the activation energies.

The main results of the IFL model are summarized in Figure 7 where the immobilized polymer fraction and its corresponding segmental dynamics are shown for different temperatures and filler fractions. In Figure 7a, f is found to span values from ca. 0.1 (6 vol.% in silica) to 0.32 (31 vol.% in silica), in qualitative agreement with rheology results.[8,9] In fact, while up to 6 vol.% in silica, the dynamical moduli (G', G'') as well as the corresponding master-curve shift factors a_T were found unchanged, a severe broadening of the whole relaxation spectrum (including the α-relaxation) was observed at 31 vol.%. More interestingly, NMR estimates of f are in fair agreement with BDS data from our previous work (f = 0.42 and 0.50 respectively).[9] We believe that the discrepancy originates from the intricate fitting procedure of BDS data, caused by the emergence of the MWS process in the same frequency window as the α-relaxation. Note that Sokolov et al. reported f=0.4 for P2VP filled with 26 vol.% in silica [14] (with slightly bigger particles R=12.5 nm), falling well in the (broad) range of immobilized layer fraction, f=0.32-0.5 (see also a summary of various systems from the same authors in Table 2 in ref.[31]). On top of this, f appears to be independent of temperature, apparently contrary to Sokolov et al. who found that f followed a (weakly) decreasing linear trend with increasing the temperature in PVAc (at similar distance from T_g than us) [18] and in P2VP and PVAc (closer to their T_g).[31] At this point, we cannot exclude that systematic deviations arise from the fact that our fitting approach only provides a reliable lower limit of f. Further efforts relying on the T_g gradient model are proposed in the next section.

Figure 7b also unambiguously reveals the slowing down of the immobilized phase relative to the bulk P2VP. The corresponding broadening of the P2VP glass transition with increasing silica content has been widely investigated through DSC and BDS, where it is treated either as the appearance of a separate relaxation assigned to the adsorbed polymer ("α_2"[14] or "α'"[17]), or a continuous gradient of mobility.[9,20] Here, LF-NMR shows a strong up-shift of τ_c when the

polymer is immobilized, with this shift being almost independent of the filler content. Quantitatively, this shift appears to be close to a decade at 473 K. This value is lower than the two decades in time reported by Holt et al. [14] (see also Bailey and Winey [32]) whereas it matches well the more recent investigations by Genix et al.,[16] both measured from BDS on similar systems. We believe that this discrepancy originates from ignoring (or limiting) the amplitude of the MWS process occurring in PNC at lower frequency than the segmental motion. In fact, this would necessitate a leftward-shift and enhance "α_2" (the immobilized segments contribution) to compensate for the lower permittivity in this frequency range.[14] Nevertheless, it is worth noting that both LF-NMR and BDS [18] indicate an unchanged temperature dependence of the segmental relaxation of bulk and interfacial P2VP segments. The corresponding activation energies range between ca. 80 and 100 kJ mol^{-1} for LF-NMR, while it is ca. twice as much in the BDS (see Figure 2). Note that no evidence for a dead layer, which would be represented by a signal contribution resembling that of bulk P2VP measured below 400 K, was found in the present work.[33,34] Further, since such nanocomposites are not expected to be thermodynamically equilibrated,[35,36] differences in the studied samples may well arise due to potential differences in preparation procedures.

This discussion to this point on the IFL model is based on the hypothesis that the segmental dynamics of the interfacial layer is isotropic ($S = 0$ in Equation 2), as in the bulk polymer. However, as reported by Sokolov et al. in refs. [12,37], it has been demonstrated that the polymer dynamic suppression at the interface is not only impacted by the strength of the interaction with the filler but also by the average local chain orientation in the vicinity of the NPs. Concretely, because the chains are expected to adopt a “pancake-like” conformation, near the NPs, their resulting segmental fluctuations become anisotropic. (Note that a similar logic can be adopted in the case of covalently grafted particles where the polymer segments close to the anchoring point would exhibit a preferred orientation normal to the NP surface). This phenomenon has been

addressed theoretically by Oyerokun and Schweizer who predicted that an anisotropic conformation increases the correlation between segmental motions (intrachain) resulting in an increase of T_g at the interface.[38]

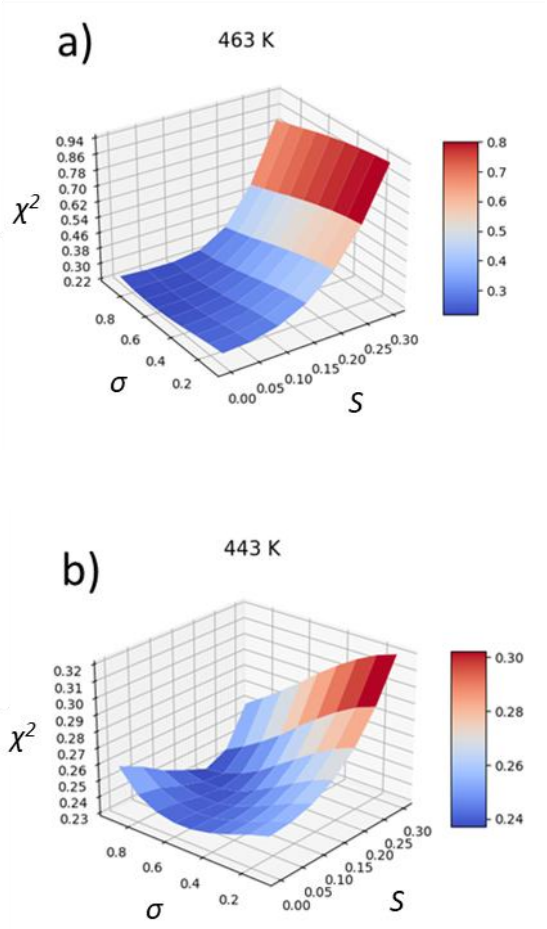

Figure 8: Fitting quality (χ^2) as a function of S and σ representing respectively the anisotropy of the segmental motion and the breadth of the segmental relaxation time distribution in the IFL model. Fits are performed on data measured on the nanocomposite loaded with 31 vol.% in silica at a) 463 K and b) 443 K.

In this context, it is logical to extend our IFL model to the case with $S \neq 0$ to check the validity of our approach, as already investigated in the past in nacre-mimetic composites [39] and semi-

crystalline polymers.[40] The result of this approach is represented in Figure 8 where the quality (χ^2) of the IFL fit is systematically plotted as function of different fixed S and σ for the 31 vol.% nanocomposite at 463 K and 443 K (the rest of the data set is presented in SI section 4). The 463 K map (Figure 8a) indicates that best fits are obtained for S close to 0 for reasonable relaxation time distributions (σ=0.6-0.8). However, this is clearly not the case for the 443 K map; rather the IFL model better describes the data for S=0.15-0.2. While this duality also emerges from the fits performed at different temperatures and filler fractions, we find more frequently that a S value significantly above 0 enhances the fitting quality. Although it is impossible at this stage to conclude quantitatively on a true value of S, these fits support the notion that the anisotropy of segmental motions is fully consistent with our LF-NMR experimental data, justifying the use of the simple IFL model in future investigations in this field.

3.3.2. NMR data fitting with the T_g gradient model

The T_g gradient model relies on the continuous variation of the glass transition temperature as a function of the distance (h) between the polymer and the filler surface. This model, successfully applied in the past by Papon et al.,[20] is employed here to fit both DSC (see Figure 2) and NMR (see Figure 6) data:

$$I_{FID,MSE}(T,t) = \frac{1}{V_{tot}} \int_{V_{tot}} I_{FID,MSE}^{P2VP}\left(T - T_g(h), t\right) dV(h) \qquad (6)$$

where $T_g(h)$ follows Equation 1 and $V_{tot} = \frac{1-\Phi}{\Phi}\frac{4}{3}\pi R^3$ is the mean polymer volume per nanoparticle. The integration is performed over spherical shells, i.e., $dV(h) = 4\pi(R+r)^2\Delta h$, up to the h value corresponding to V_{tot}. To apply this fitting method to NMR data, we choose $I_{FID,MSE}^{P2VP}\left(T - T_g(h), t\right)$ to follow the AW expression (Equation 3) as this function successfully fits the whole neat P2VP data set (see Figure 3). Our conclusions will thus be independent of the

failure of the AW approach to provide a fully quantitative τ_c, as we ultimately model the composite data as a superposition of temperature-shifted neat-P2VP responses (see ref.[20]). Practically, the continuous integration in Equation 6 is implemented as a discrete sum of the neat P2VP signals in spherical shells at distance h from the surface and thickness Δh. Neat signals were measured every 10 K between 413 K and 473 K. The only fitting parameters are δ (appearing in the expression of $T_g(h)$) and possibly β when it is not forced to be 1. Note that this "slicing" method was also used by Papon in the Equation 6 of ref.[20] to incorporate a maximum shifted-T_g cutoff. The glass transition temperature profile resulting from the fit performed on the 31 vol.% nanocomposite NMR data at T=453 K is provided in Figure 9 as a decreasing function (Equation 1) with $\delta = 0.024$ nm ($\beta = 1$). This value is found to vary slightly between 0.017 and 0.025 nm when changing the temperature from 443 to 473 K, supporting the consistency of the T_g gradient model. Corresponding fits are displayed in Figure 9b-c. In the same interval of (trustworthy) temperatures, the 18 vol.% nanocomposite data fitting results in δ varying between 0.01 nm and 0.025 ($\beta = 1$). The analogous values for the 10 vol.% composite, for which the NMR signal is very close to the neat P2VP one, are in the 0.04-0.045 nm interval. Although δ values for 10 and 18 vol.% are thus in fair agreement with the 31 vol.% sample, we believe that the results extracted from the latter sample are more accurate because of a larger fraction of immobilized layer. Overall, $\delta \approx 0.025$ emerges from the T_g gradient model, with no significant improvement of the fit when β is varied in the 0.8-1.5 range.

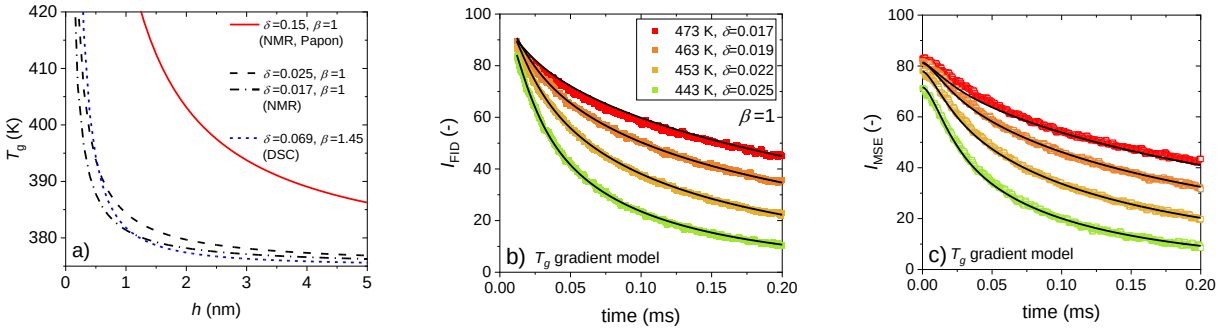

Figure 9: T_g profile as a function of the distance from the filler surface (h) resulting from the T_g gradient model applied to the whole set of DSC data (short-dashed blue line) and NMR (dashed black line) data from the nanocomposite loaded with 31 vol.% in silica at 453 K. Results from Papon et al. are displayed as a solid red line. b-c) Corresponding FID and MSE-FID data jointly fitted with the T_g gradient model (black solid lines) in the sensitive temperature range. Corresponding δ values belong to the intervals 0.029-0.047 and 0.01-0.026 for Φ=10 vol.% and 18 vol.% respectively. Variations are erratic with the temperature.

As presented in Figure 2, the T_g gradient model can also be used to rationalize successfully DSC data. In this case we performed the simultaneous fit on the whole data set ($C_p = f(T)$ measurements). Practically, the situation is different from the previous (NMR) case since the data are obtained from a continuous variation of temperature (it is every 10 K in NMR). This results is defining somehow arbitrarily the thickness of the slices (Δh) considered for the fitting, each slice being characterized by a DSC profile identical to the neat P2VP one, but shifted "diagonally" by 10 K along the line defining the $C_p(T)$ in the glassy regime (see Figure 2a inset). Several fits were performed assuming Δh=0.1, 0.2 and 0.5 nm, but they provided a similar if not identical result: $\delta \approx 0.069$ with $\beta \approx 1.45$. (This is as expected.) The corresponding T_g profile is

reported in Figure 9 for comparison with its NMR counterpart and previous NMR data by Papon et al. on PEA where larger silica particles were used.[20]

The main message provided by Figure 9 is that the T_g gradient model can be used successfully on both NMR and DSC data providing similar T_g profiles; our analysis procedure is thus quite robust. We believe that the slight discrepancies in δ ($0.025\ vs.\ 0.069$) and β ($1\ vs.\ 1.45$) are due to the simplicity of the model, notably Equation 1 and the constancy of other parameters of the Vogel-Fulcher relation, and the uncertainties in the experimental data. In other words, although we cannot use directly the exact values of the "intermediate parameters" δ and β obtained from DSC to fit NMR data, the two resulting T_g profiles calculated through Equation 1 and should be seen as the main output describing the materials, do look very similar. Besides, it is worth noting that investigating silica/PEA PNCs in the same manner, Papon et al. found $\delta = 0.15$ nm, *i.e.*, a much larger characteristic distance than in the present study (see Figure 9). We assign this difference to a particle size effect: Papon et al. dealt with particles of radius 21.5 nm while it is only 7 nm in our case. In fact, reducing the NP radius reduces the thickness of the "slowed down" polymer layer. In ref.[7], Harton et al. reported a slowed down polymer layer thickness of 1 nm in P2VP/silica PNCs containing particles or 15 nm diameter (*i.e.*, identical to the present work); this is in excellent agreement with the T_g profile we report in Figure 9. On the other hand, they showed that this thickness could reach ca. 5 nm (closer to the Papon et al. profile in Figure 9) in the case of a flat interface.

Apart from specific surface considerations, other authors showed the impact of the mean surface-to-surface distance between two adjacent NPs. Chen et al.[8] notably showed the formation of "glassy bridges" for particles of 7 nm radius from $\Phi = 10$ vol.%, while this threshold was shifted to ca. 45 vol.% with particles of 25 nm radius.[8] In agreement with these results, Baeza et al. found a (progressive) dynamical transition from WLF to Arrhenius behavior when the filler content was increased in identical materials.[9] Finally, Cheng et al. also demonstrated

the significant effect of reducing the interparticle distance on the polymer segmental motion by using small NPs (R=2 nm).[41]

At last, we want to highlight that although Equation 6 is expected to fail for very high filler fractions resulting in an overlap of the slowdown polymer shells surrounding the NPs, this hypothesis is not relevant in the present paper. In fact, the average wall-to-wall interparticle distance, approximated by $d_{IP} = \left(\left(\frac{16}{\pi\Phi}\right)^{1/3} - 2\right)$, is 12.0, 7.3 and 3.8 nm respectively for Φ = 10, 18 and 31 vol.%. These distances must be compared with the shape of the T_g gradient presented in Figure 9, clearly showing that no significant slowdown happens beyond 2 nm, confirming therefore that Equation 6 is consistent to describe our data.

4. Conclusions

LF-NMR relaxometry experiments have been performed on P2VP/silica attractive nanocomposites with varying the filler fraction (6-31 vol.%) and temperature (423-473 K) with the aim of investigating the immobilized polymer chains, both in terms of fraction and dynamical slow down. Two approaches have been critically examined to fit the whole data set: (i) the single interfacial layer model (IFL) and (ii) the T_g gradient model. In the former case, the immobilized layer is seen as a single shell within which the segmental relaxation time follows a log-normal distribution while in the latter case the polymer T_g is taken to continuously increase as one proceeds closer to the filler surface, resulting in polymer "slices" of increasing relaxation time. In qualitative agreement with previous BDS investigations, we show in the present work that both approaches can be implemented to fit successfully NMR data. Quantitatively, our NMR analyses support the finding of Genix et al.[16] who evaluate recently the dynamical slowdown of the interfacial layer to be ca. 1 decade on average by means of BDS and Brillouin light scattering.

However, they are in contrast with the earlier work of Holt et al.[14] who found a 2-decades slowdown with BDS in similar systems – pointing the difficulties to fit unequivocally BDS data.

The discrimination between the IFL and the T_g gradient approaches becomes possible only when applying these models to fit previously measured DSC data. Obviously, the IFL model cannot fit the heat capacity of the polymer phase in PNCs as convincingly as the T_g gradient model (with consistent outputs with respect to NMR data). However, it is worth noting that the implementation of the IFL model is also compatible with the existence of anisotropic segmental motions at the interface with the filler making the two approaches complementary to describe the whole material's physics. This phenomenon, as well as related changes in NMR T_2 relaxation, can also explain reduced fitting quality and fitting bias resulting in slight discrepancies in the T_g gradient model (while NMR gives β =1, DSC suggests β =1.45).

Apart from rheology, BDS, DSC and NMR, other techniques such as X-ray photoelectron spectroscopy (XPS) and Sum Frequency Generation (SFG) were recently used to complement the information about the immobilized polymer.[42] Further methods enabling the characterization of local and collective dynamics of nanofilled polymers are discussed in a recent review by Bailey and Winey.[32] The unification of experimental results coming from these various probes (including numerical simulations) appears as a central challenge for the coming years.

Associated content

Supplementary Information: (1) Thermogravimetric analysis on the neat P2VP, and nanocomposites loaded with 10, 30 and 50 wt.% in silica. (2) M_2 determination from low temperature experiments on the neat P2VP. (3) All FID and MSE-FID "raw" signals measured from the whole set of samples. (4) Additional fitting maps $\chi^2 = f(S, \sigma)$ for the IFL model.

Author Information

Corresponding authors:

Guilhem P. Baeza, guilhem.baeza@insa-lyon.fr - 0000-0002-5142-9670

Kay Saalwächter, kay.saalwaechter@physik.uni-halle.de - 0000-0002-6246-4770

Notes: The authors declare no competing financial interest.

Acknowledgements

All the authors warmly thank Walter Chassé (Univ. Munster) for its help with the LF-NMR routine and Paul Sotta (INSA-Lyon) for technical support on the minispec. The authors also thank Ahmed Belhadj and Pierre Alcouffe (INSA-Lyon and Univ. Lyon 1, respectively) for the TGA and TEM measurements. TEM was performed at the "Centre Technologique des Microstructures" at University of Lyon 1. G.P.B. thanks Aurélien Doitrand (INSA-Lyon) for his help with the IFL model fitting implementation.

Funding sources

G.P.B. acknowledges the financial support of IDEX-Lyon and INSA Lyon through the program ELAN-ERC as well as the Institut Carnot I@L for the funding assigned to the project POMMADE.

References

1. Sanchez, C., Julián, B., Belleville, P. & Popall, M., Applications of hybrid organic–inorganic nanocomposites. *Journal of Materials Chemistry* **15**, 2005, 3559.
2. Ray, S. S. & Okamoto, M., Polymer/layered silicate nanocomposites: a review from preparation to processing. *Progress in polymer science* **28**, 2003, 1539.
3. Schadler, L. S., Kumar, S. K., Benicewicz, B. C., Lewis, S. L. & Harton, S. E., Designed interfaces in polymer nanocomposites: A fundamental viewpoint. *MRS bulletin* **32**, 2007, 335.
4. Kumar, S. K., Benicewicz, B. C., Vaia, R. A. & Winey, K. I., 50th anniversary perspective: are polymer nanocomposites practical for applications? *Macromolecules* **50**, 2017, 714.
5. Zhang, P., Morris, M. & Doshi, D., Materials development for lowering rolling resistance of tires. *Rubber Chemistry and Technology* **89**, 2016, 79.
6. Mujtaba, A., Keller, M., Ilisch, S., Radusch, H. J., Beiner, M., Thurn-Albrecht, T., & Saalwachter, K., Detection of surface-immobilized components and their role in viscoelastic reinforcement of rubber–silica nanocomposites. *ACS Macro letters* **3**, 2014, 481.
7. Harton, S. E., Kumar, S. K., Yang, H., Koga, T., Hicks, K., Lee, H., Mijovic, J., Liu, M., Vallery, R. S., & Gidley, D. W., Immobilized polymer layers on spherical nanoparticles. *Macromolecules* **43**, 2010, 3415.
8. Chen, Q., Gong, S., Moll, J., Zhao, D., Kumar, S. K., & Colby, R. H., Mechanical reinforcement of polymer nanocomposites from percolation of a nanoparticle network. *ACS Macro Letters* **4**, 2015, 398.
9. Baeza, G. P., Dessi, C., Costanzo, S., Zhao, D., Gong, S., Alegria, A., Colby, R. H., Rubinstein, M., Vlassopoulos, D., & Kumar, S. K., Network dynamics in nanofilled polymers. *Nature communications* **7**, 2016, 1.
10. Baeza, G. P., Genix, A. C., Degrandcourt, C., Petitjean, L., Gummel, J., Couty, M., & Oberdisse, J., Multiscale Filler Structure in Simplified Industrial Nanocomposite Silica/SBR Systems Studied by SAXS and TEM. *Macromolecules* **46**, 2013, 317.
11. Mujtaba, A., Keller, M., Ilisch, S., Radusch, H. J., Thurn-Albrecht, T., Saalwachter, K., & Beiner, M., Mechanical properties and cross-link density of styrene–butadiene model composites containing fillers with bimodal particle size distribution. *Macromolecules* **45**, 2012, 6504.
12. Popov, I., Carroll, B., Bocharova, V., Genix, A. C., Cheng, S., Khamzin, A., Kisliuk, A., & Sokolov, A. P., Strong Reduction in Amplitude of the Interfacial Segmental Dynamics in Polymer Nanocomposites. *Macromolecules* **53**, 2020, 4126.
13. Yang, J., Melton, M., Sun, R., Yang, W. & Cheng, S., Decoupling the polymer dynamics and the nanoparticle network dynamics of polymer nanocomposites through dielectric spectroscopy and rheology. *Macromolecules* **53**, 2019, 302.

14. Holt, A. P., Griffin, P. J., Bocharova, V., Agapov, A. L., Imel, A. E., Dadmun, M. D., Sangoro, J. R., & Sokolov, A. P., Dynamics at the polymer/nanoparticle interface in poly (2-vinylpyridine)/silica nanocomposites. *Macromolecules* **47**, 2014, 1837.

15. Gong, S., Chen, Q., Moll, J. F., Kumar, S. K. & Colby, R. H., Segmental dynamics of polymer melts with spherical nanoparticles. *ACS Macro Letters* **3**, 2014, 773.

16. Genix, A. C., Bocharova, V., Kisliuk, A., Carroll, B., Zhao, S., Oberdisse, J., & Sokolov, A. P., Enhancing the mechanical properties of glassy nanocomposites by tuning polymer molecular weight. *ACS applied materials & interfaces* **10**, 2018, 33601.

17. Cheng, S., Holt, A. P., Wang, H., Fan, F., Bocharova, V., Martin, H., Etampawala, T., White, T. B., Saito, T., Kang, N.-G., Dadmun, M. D., Mays, J. W., & Sokolov, A. P., Unexpected molecular weight effect in polymer nanocomposites. *Physical review letters* **116**, 2016, 038302.

18. Cheng, S. & Sokolov, A. P., Correlation between the temperature evolution of the interfacial region and the growing dynamic cooperativity length scale. *The Journal of Chemical Physics* **152**, 2020, 094904.

19. Papon, A., Saalwächter, K., Schäler, K., Guy, L., Lequeux, F., & Montes, H., Low-field NMR investigations of nanocomposites: polymer dynamics and network effects. *Macromolecules* **44**, 2011, 913.

20. Papon, A., Montes, H., Hanafi, M., Lequeux, F., Guy, L., & Saalwächter, K., Glass-transition temperature gradient in nanocomposites: evidence from nuclear magnetic resonance and differential scanning calorimetry. *Physical review letters* **108**, 2012, 065702.

21. Keddie, J. L., Jones, R. A. & Cory, R. A., Size-dependent depression of the glass transition temperature in polymer films. *EPL (Europhysics Letters)* **27**, 1994, 59.

22. Maus, A., Hertlein, C. & Saalwächter, K., A robust proton NMR method to investigate hard/soft ratios, crystallinity, and component mobility in polymers. *Macromolecular Chemistry and Physics* **207**, 2006, 1150.

23. Anderson, P.-W. & Weiss, P., Exchange narrowing in paramagnetic resonance. *Reviews of Modern Physics* **25**, 1953, 269.

24. Szymoniak, P., Qu, X., Abbasi, M., Pauw, B. R., Henning, S., Li, Z., Wang, D.-Y., Schick, C., Saalwächter, K., & Schönhals, A., Spatial inhomogeneity, Interfaces and Complex Vitrification Kinetics in a Network Forming Nanocomposite. *Soft Matter* **17**, 2021, 2775.

25. Liu, G., Cheng, H., Yan, L. & Zhang, G., Study of the kinetics of the pancake-to-brush transition of poly (N-isopropylacrylamide) chains. *The Journal of Physical Chemistry B* **109**, 2005, 22603.

26. Ou-Yang, H. D. & Gao, Z., A pancake-to-brush transition in polymer adsorption. *Journal de Physique II* **1**, 1991, 1375.

27. Beiner, M., Relaxation in poly (alkyl methacrylate) s: crossover region and nanophase separation. *Macromolecular rapid communications* **22**, 2001, 869.

28. Arbe, A., Genix, A.-C., Arrese-Igor, S., Colmenero, J. & Richter, D., Dynamics in poly (n-alkyl methacrylates): A neutron scattering, calorimetric, and dielectric study. *Macromolecules* **43**, 2010, 3107.

29. Papadopoulos, P., Peristeraki, D., Floudas, G., Koutalas, G. & Hadjichristidis, N., Origin of glass transition of poly (2-vinylpyridine). A temperature-and pressure-dependent dielectric spectroscopy study. *Macromolecules* **37**, 2004, 8116.

30. Wind, M., Graf, R., Heuer, A. & Spiess, H. W., Structural relaxation of polymers at the glass transition: Conformational memory in poly (n-alkylmethacrylates). *Physical review letters* **91**, 2003, 155702.

31. Cheng, S., Carroll, B., Lu, W., Fan, F., Carrillo, J. M. Y., Martin, H., Holt, A. P., Kang, N.-G., Bocharova, V., Mays, J. W., Sumpter, B. G., Dadmun, M. & Sokolov, A. P., Interfacial properties of polymer nanocomposites: Role of chain rigidity and dynamic heterogeneity length scale. *Macromolecules* **50**, 2017, 2397.

32. Bailey, E. J. & Winey, K. I., Dynamics of Polymer Segments, Polymer Chains, and Nanoparticles in Polymer Nanocomposite Melts: A Review. *Progress in Polymer Science*, 2020, 101242.

33. Napolitano, S. & Wübbenhorst, M., Dielectric signature of a dead layer in ultrathin films of a nonpolar polymer. *The Journal of Physical Chemistry B* **111**, 2007, 9197.

34. Napolitano, S., Pilleri, A., Rolla, P. & Wubbenhorst, M., Unusual deviations from bulk behavior in ultrathin films of poly (tert-butylstyrene): Can dead layers induce a reduction of T g? *Acs Nano* **4**, 2010, 841.

35. Oh, S. M., Abbasi, M., Shin, T. J., Saalwächter, K. & Kim, S. Y., Initial solvent-driven nonequilibrium effect on structure, properties, and dynamics of polymer nanocomposites. *Physical review letters* **123**, 2019, 167801.

36. Genix, A. C., Bocharova, V., Carroll, B., Lehmann, M., Saito, T., Krueger, S., He, L., Dieudonné-George, P., Sokolov, A. P., & Oberdisse, J., Understanding the static interfacial polymer layer by exploring the dispersion states of nanocomposites. *ACS applied materials & interfaces* **11**, 2019, 17863.

37. Holt, A. P., Bocharova, V., Cheng, S., Kisliuk, A. M., White, B. T., Saito, T., Uhrig, D., Mahalik, J. P., Kumar, R., Imel, A. E., Etampawala, T., Martin, H., Sikes, N., Sumpter, B. G., Dadmun, M. D., & Sokolov, A. P., Controlling interfacial dynamics: covalent bonding versus physical adsorption in polymer nanocomposites. *ACS nano* **10**, 2016, 6843.

38. Oyerokun, F. T. & Schweizer, K. S. Theory of glassy dynamics in conformationally anisotropic polymer systems. *The Journal of chemical physics* **123**, 2005, 224901.

39. Eckert, A., Abbasi, M., Mang, T., Saalwächter, K. & Walther, A., Structure, Mechanical Properties, and Dynamics of Polyethylenoxide/Nanoclay Nacre-Mimetic Nanocomposites. *Macromolecules* **53**, 2020, 1716.

40. Kurz, R., Achilles, A., Chen, W., Schäfer, M., Seidlitz, A., Golitsyn, Y., Kressler, J., Paul, W., Hempel, G., Miyoshi, T., Thurn-Albrecht, T., & Saalwächter, K., Intracrystalline jump motion in poly (ethylene oxide) lamellae of variable thickness: A comparison of NMR methods. *Macromolecules* **50**, 2017, 3890.

41. Cheng, S., Xie, S. J., Carrillo, J. M. Y., Carroll, B., Martin, H., Cao, P. F., Dadmun, M. D., Sumpter, B. G., Novikov, V. N., Schweizer, K. S., & Sokolov, A. P., Big effect of small nanoparticles: a shift in paradigm for polymer nanocomposites. *ACS nano* **11**, 2017, 752.

42. Voylov, D. N., Holt, A. P., Doughty, B., Bocharova, V., Meyer III, H. M., Cheng, S., Martin, H., Dadmun, M., Kisliuk, A., & Sokolov, A. P. Unraveling the molecular weight dependence of interfacial interactions in poly (2-vinylpyridine)/silica nanocomposites. *ACS Macro Letters* **6**, 2017, 68.

TABLE OF CONTENT

T_g Gradient vs. Single Interfacial Layer:

On the Immobilized Polymer Fraction in Attractive Nanocomposites

Carlos Fernandez de Alba, Andrew M. Jimenez, Mozhdeh Abbasi,
Sanat K. Kumar, Kay Saalwächter and Guilhem P. Baeza

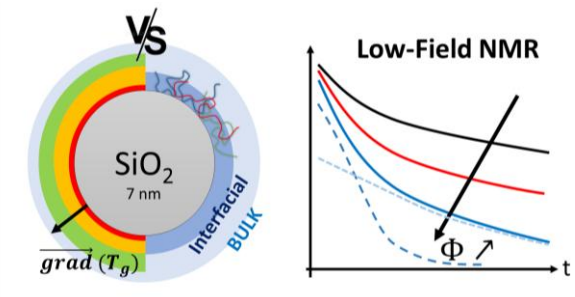

For Table of Contents use only (4*8 cm)